Pilot Allocation and Computationally Efficient Non-Iterative Estimation of Phase Noise in OFDM

Pilot Allocation and Computationally Efficient Non-Iterative Estimation of Phase Noise in OFDM

Ville Syrjälä, Toni Levanen, Tero Ihalainen, and Mikko Valkama

Abstract—**This paper proposes a pilot subcarrier allocation approach for OFDM systems, which enables construction of symbol-wise phase-noise estimates with high efficiency and low overhead in a non-iterative manner. The complexity and performance of the overall phase-noise suppression algorithm together with the proposed pilot allocation approach are evaluated in 5G SU-MIMO and MU-MIMO radio links at 28 GHz carrier frequency, showing clear complexity-performance benefits against a state-of-the-art reference algorithm.**

Index Terms—**OFDM, reference signals, MIMO, phase noise, ICI, mitigation, computational complexity, cmW, mmW, 5G.**

I. INTRODUCTION

$\mathbf{P}$HASE noise (PN) has serious inband effects in orthogonal frequency division multiplexing (OFDM) systems [1] which can be divided into two parts. The first is called common phase error (CPE), which corresponds to PN-dependent common rotation at every subcarrier within an OFDM symbol, which is typically mitigated by using pilot subcarriers [2]. The second effect stemming from the spread of the energy of each subcarrier on top of the other subcarriers is called inter-carrier interference (ICI), which in turn is much more complex in nature [1], [2].

In the literature, considerable amount of research has focused on ICI mitigation, e.g., [2]-[7]. Despite this, compact transceiver implementations with limited computational resources still rely on good quality oscillators instead of actually mitigating the ICI with signal processing. However, cheap oscillators working at high frequencies require that the ICI is handled with signal processing, because the PN problem gets substantially more challenging at centimeter wave (cmW) and millimeter wave (mmW) frequencies, where, e.g., the emerging new 5G systems will operate [8]. OFDM systems using high-order modulation and coding schemes (MCS) are very sensitive to PN and thus require advanced PN compensation solutions. In future 5G networks, also the processing delay requirements will become stricter, limiting, e.g., the use of iterative PN compensation approaches.

In this paper, we introduce a pilot allocation strategy that enables non-iterative, computationally effective, but accurate estimation and suppression of PN induced CPE and ICI, with low latency and low overhead. The accurate estimation and suppression of PN enables the use of higher-order MCSs allowing significantly improved spectral efficiency, particularly at higher cmW or mmW bands. No prior symbol decisions or information about consecutive OFDM symbols are needed, resulting in low latency and reduced buffering requirements. The block-wise pilot signal design, with the defined estimation and compensation

V. Syrjälä, T. Levanen and M. Valkama are with Tampere University of Technology, Tampere, Finland (e-mail: ville.syrjala@tut.fi).
T. Ihalainen is with the Nokia Bell Labs, Tampere, Finland.

algorithms, can be applied to single-input single-output (SISO), single-user (SU) multiple-input multiple-output (MIMO), and multi-user (MU)-MIMO OFDM links.

II. OFDM RADIO LINK MODEL WITH PHASE NOISE

Assuming that the channel delay spread is shorter than the utilized cyclic prefix length, the demodulated received OFDM signal corrupted by receiver side PN can be written as [2]

$$R_k = X_k H_k J_0 + \sum_{l=0, l \neq k}^{N-1} X_l H_l J_{k-l} + Z_k, \, k \in 0, \dots, N-1 \,, \quad (1)$$

where k is the subcarrier index, X_k is the subcarrier transmit symbol, H_k is the channel frequency response, Z_k is the discrete Fourier transformed white Gaussian noise, and J_l is the discrete Fourier transformed PN complex exponential expressed as

$$J_l = \frac{1}{N} \sum_{n=0}^{N-1} e^{j\phi_n} e^{-\frac{j2\pi nl}{N}} \,. \quad (2)$$

Here ϕ_n is the sampled time-varying PN within the considered OFDM symbol. Notice that the model is written for an arbitrary OFDM symbol, and thus the OFDM symbol index has been omitted for simplicity. In the first term of (1), the effect of the CPE is visible as a multiplication by J_0, while the second additive term corresponds to the effect of the ICI [2]. As shown in [2], the model in (1)-(2) describes a PN-impaired OFDM radio link very accurately also in cases where both the transmitter and receiver side PN sources are significant.

III. PHASE NOISE MITIGATION

A. Reference Frequency-Domain Suppression Strategy

If we rewrite (1) into a form where only $2u+1$ centermost frequency bins of the PN complex exponential are assumed significant, i.e., we exploit the strong lowpass nature of the PN process, we arrive into a form [2]

$$R_k = \sum_{l=-u}^{u} X_{k-l} H_{k-l} J_l + Q_k = \sum_{l=-u}^{u} Y_{k-l} J_l + Q_k \,. \quad (3)$$

Here, Q_k includes ICI from the non-significant frequency bins of the PN complex exponential and the additive noise. Then, for a set of subcarriers $k \in \{l_1, l_2, \dots, l_p\}: \, p \geq 2u+1$, we can write a set of linear equations as [2]

$$\begin{bmatrix} R_{l_1} \\ R_{l_2} \\ \vdots \\ R_{l_p} \end{bmatrix} = \begin{bmatrix} Y_{l_1+u} & Y_{l_1+u-1} & \cdots & Y_{l_1-u} \\ Y_{l_2+u} & \ddots & \ddots & Y_{l_2-u} \\ \vdots & \ddots & \ddots & \vdots \\ Y_{l_p+u} & \cdots & \cdots & Y_{l_p-u} \end{bmatrix} \begin{bmatrix} J_{-u} \\ J_{-u+1} \\ \vdots \\ J_u \end{bmatrix} + \begin{bmatrix} Q_{l_1} \\ Q_{l_2} \\ \vdots \\ Q_{l_p} \end{bmatrix} \Leftrightarrow \quad (4)$$

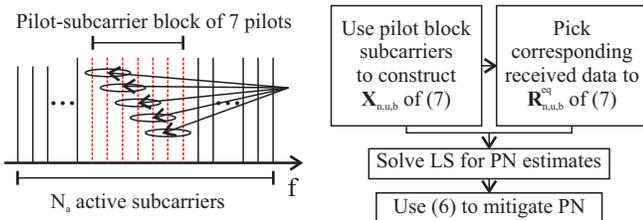$$\mathbf{R}_p = \mathbf{Y}_{u,p} \mathbf{J}_u + \mathbf{Q}_p \,.$$

Fig. 1. An example pilot subcarrier block and the groups of $2u+1$ pilots to solve (7), indicated by circles and arrows, for the case of $u = 1$. We have pilot subcarrier block of size $b = 7$, and therefore a system of $b-2u = 5$ equations in (7). Also, the basic flow diagram of the algorithm is depicted.

Now, if we assume that the values of $\mathbf{Y}_{u,p}$ are known, we can obtain the estimate of $\mathbf{J}_u$ with least squares (LS) approach as [3]

$$\hat{\mathbf{J}}_u \triangleq [\hat{J}_{-u}, \ldots, \hat{J}_u]^T = (\mathbf{Y}_{u,p}^H \mathbf{Y}_{u,p})^{-1} \mathbf{Y}_{u,p}^H \mathbf{R}_p, \qquad (5)$$

where $(\cdot)^T$ and $(\cdot)^H$ denote the transpose and conjugate transpose, respectively. The LS solution is computationally relatively simple, while also the corresponding minimum mean square error (MMSE) solution is formulated in [2]. Algorithms, e.g., in [2], [3], and [4] exploit (4) in decision feedback manner for PN estimation. The suppression of PN is then done by deconvolution [2], and the signal after PN suppression can be written as

$$\hat{Y}_k = \sum_{l=-u}^{u} R_{k-l} \hat{J}_{-l}^*. \qquad (6)$$

Here x^* denotes the complex conjugate of x, and the deconvolution needs to be done only for the active subcarriers.

B. Proposed Method

Here pilot subcarrier allocation schemes are proposed, which allow us to formulate the non-iterative PN estimation and suppression algorithm with very low computational complexity. After the channel estimation and equalization, both the CPE and ICI are estimated simultaneously without data symbol detection or iterations, and without any information of the consecutive OFDM symbols. This results in very low processing latency, complexity and buffering requirements. After the estimation, the PN is suppressed with deconvolution, as formulated in (6). The flow diagram of the algorithm is depicted in Fig. 1.

The proposed pilot subcarrier structure is based on the set of linear equations in (4). To solve the LS estimate of the $2u+1$ frequency bins of PN in (5), we need to know at least $2u+1$ different values of Y_k, and neighborhood of u values on both sides of each of these. The key observation is that the neighborhoods can be overlapping, so we can *reuse most of the values in the adjacent neighborhoods* in the estimation process (see Fig. 1). To carry out the PN estimation based on the above idea, the smallest required block size is only $4u+1$ adjacent values of Y_k. If the size of the subcarrier block is $b \geq 4u+1$ and the index of the first subcarrier in the block is n, then the set of linear equations for the channel equalized received signal reads

$$\begin{bmatrix} R_{n+u}^{eq} \\ R_{n+u+1}^{eq} \\ \vdots \\ R_{n+b-u-1}^{eq} \end{bmatrix} = \begin{bmatrix} X_{n+2u} & X_{n+2u-1} & \cdots & X_n \\ X_{n+2u+1} & \ddots & \ddots & X_{n+1} \\ \vdots & \ddots & \ddots & \vdots \\ X_{n+b-1} & \cdots & \cdots & X_{n+b-2u-1} \end{bmatrix} \begin{bmatrix} J_{-u} \\ J_{-u+1} \\ \vdots \\ J_u \end{bmatrix} + \begin{bmatrix} Q_{n+u}^{eq} \\ Q_{n+u+1}^{eq} \\ \vdots \\ Q_{n+b-u-1}^{eq} \end{bmatrix} \Leftrightarrow$$

$$\mathbf{R}_{n,u,b}^{eq} = \mathbf{X}_{n,u,b} \mathbf{J}_u + \mathbf{Q}_{n,u,b}^{eq}. \qquad (7)$$

Here, Q_n^{eq} contains residual noise and ICI after the channel equalization. Then, the PN can be estimated with LS estimation from (7) as $\hat{\mathbf{J}}_u = (\mathbf{X}_{n,u,b}^H \mathbf{X}_{n,u,b})^{-1} \mathbf{X}_{n,u,b}^H \mathbf{R}_{n,u,b}^{eq}$. To obtain the required block of X_k values in (7) without decision feedback iterations, we propose to use a block of contiguous pilot subcarriers, as illustrated in Fig. 1. Overall, the proposed pilot block structure has a reasonable overhead to facilitate highly efficient symbol-by-symbol CPE and ICI estimation in modern communications systems utilizing thousands of subcarriers. Since most of the PN energy is at the low frequencies, even very small values of u, e.g., $u = 1$ or $u = 2$, and thus small block size, give significant performance gains [2], [3]. Notice, however, that if we increase the pilot subcarrier block size from the minimum of $4u+1$, the estimation accuracy can be improved at the cost of increased pilot overhead, as will be shown in Section V.

Utilization of a single block of pilot subcarriers is the most spectrally efficient solution. However, frequency diversity can be attained by using multiple pilot subcarrier blocks. The size of each block should always be at least $2u+1$ subcarriers. If we want to divide the needed subcarriers into $a > 1$ separate groups of adjacent pilot subcarriers, we need at least $2au + 2u + 1$ pilot subcarriers to carry out the PN estimation. Every additional separate pilot block always requires $2u$ more pilots for the PN estimation.

The rest of the paper focuses on the case of a single block of pilot subcarriers for minimal overhead. The overhead and its impact on the throughput are further discussed in Section V. For clarity, we also state that separate channel estimation pilots are assumed.

C. Complexity Analysis of Proposed Algorithm

The complexity of the proposed algorithm is very low. No separate CPE compensation is needed, as it is compensated by the proposed algorithm simultaneously with the ICI. The complexity of the proposed algorithm is dominated by the complexity of the LS estimation and the complexity of PN mitigation by deconvolution. For the deconvolution, the complexity is $2u+1$ complex multiplications per data-carrying active subcarrier for which the PN compensation is applied. For the LS estimation, the complexity is

$$8u^2 p + 10up + 3p + 8u^3 + 12u^2 + 6u + 1 \qquad (8)$$

complex multiplications. As an example, if $u = 1$ and we have $p = 9$ pilots, and therefore a set of 7 linear equations to solve, we have 216 complex multiplications per OFDM symbol. With the proposed algorithm, for OFDM symbols with high number of active subcarriers, the deconvolution is dominating from the complexity point of view, but for smaller amounts of active scheduled data subcarriers the complexity of the LS estimation becomes dominating. The state-of-the-art reference technique of [2] has the same amount of multiplications in terms of the parameters in (8), but in practice comparable estimation performance is obtained with 3 iterations, p of 16 and u of 3. Already a single iteration results in 2023 complex multiplications per OFDM symbol, and if iterated further, the complexity gets multiplied. These values of p and u are used also in the performance comparisons provided in Section V. Notice, that the reference algorithm from [2] requires also symbol decisions which significantly increases the complexity and the latency, especially with higher-order modulations.
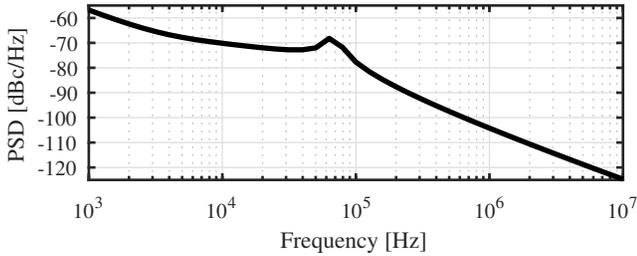
Fig. 2. The power spectral density (PSD) of the PN of the used oscillators.

IV. PHASE NOISE MITIGATION STRATEGY IN MIMO-OFDM

The proposed algorithm can be used also in MIMO links. It is reasonable to assume that in small mobile transceivers a common oscillator is shared between the antennas, so the PN realization is always the same for each antenna port. In SU-MIMO, when the same pilot subcarrier block for PN estimation is sent from all the antenna ports of the transmitter, the received pilot blocks can be averaged across the received streams after the channel equalization, and the PN estimation can then be carried out. This is beneficial, because of relatively low complexity compared to stream-by-stream estimation of the PN and reduced noise variance. It is also possible to transmit the PN estimation pilots only from a single antenna port to reduce the pilot overhead. In this case, the averaging gain is lost and the PN estimation accuracy is defined by the inter-stream-interference level in high SNR regime.

In multi-user uplink (UL), each user equipment (UE) requires their own PN pilot block, because each UE has an independent PN realization. Averaging the PN pilots over all streams from one UE is possible, assuming that one oscillator is shared by all the transmit antenna ports in the UE, and that each UE transmits the PN pilot block in all streams. Sharing the same time-frequency resources by each UE in MU-MIMO is beneficial, because the interfering signal from each UE is known. If different resources are used, the PN pilot block of the desired UE is interfered by a random data by other UEs, unless the corresponding subcarriers are muted by other UEs.

V. SIMULATION RESULTS AND ANALYSIS

A. Simulation Scenario and Simulator Description

The studied scenario follows closely the 3GPP 5G New Radio (NR) physical layer standardization in [9], [10], and thus represents a very timely example. In the simulator, an OFDM signal is generated with fast Fourier transform (FFT) length of 2048 and with 1284 active subcarriers. For the active subcarriers, 64QAM is used as a representative example of fairly high modulation order. The center frequency is 28 GHz, and the subcarrier spacing is 60 kHz, while the total carrier bandwidth is 80 MHz. We use cyclic prefix of 144 samples (at baseband sampling rate of 122.88 MHz). We incorporate both the transmitter and receiver PNs that are generated by a charge-pump PLL oscillator [11] tuned to give similar power spectral density as used in 5G standardization evaluations [12], with PSD shown in Fig. 2. The radio channel modeling is based on the clustered delay line (CDL) C and D multipath channel models [13]. The non-line-of-sight (NLOS) CDL-C and line-of-sight (LOS) CDL-D channels are with the root-mean-squared (RMS) delay spreads of 300 ns and

50 ns, respectively. In the CDL-D channel, the K-factor is 9 dB. These are selected since they correspond to evaluation assumptions for cmW radio link performance in 5G standardization [9]. CDL-D 50 ns and CDL-C 300 ns offer typical small cell LOS and NLOS evaluation cases, respectively [9]. Per polarization, 8x8 antenna array is assumed at the BS and 2x2 array at the UE [9]. Different polarizations are used for different spatial MIMO streams. A 5G NR like subframe structure consisting of 14 OFDM symbols is assumed, where the first two symbols are reserved for control. From the remaining 12 symbols, three equally spaced symbols dedicated for demodulation reference signals are used for channel estimation and the rest carry user data and PN estimation pilots. In each OFDM symbol carrying user data, a contiguous block of b pilot subcarriers (proposed method) or 24 scattered, equidistant pilot subcarriers (reference methods) are allocated for PN estimation. The actual channel estimation is based on the well-known MMSE solution. The channel estimates are interpolated in time and frequency by using a Wiener interpolator after which a subcarrier wise MMSE equalizer is applied on the data subcarriers, prior to PN mitigation. The radio link performance is evaluated by block-error ratio (BLER) and throughput. BLER target of 10% is assumed, which is common in mobile radio networks using hybrid automatic repeat request (HARQ) on top of the channel coding.

The studied cases are: 1) 'No PN' case, where no PN nor pilots are added, 2) 'CPE m.' case, where only CPE is mitigated [2], 3) 'Pet' case where, CPE and ICI are mitigated in a way proposed in [2] and 4) '$u;b$' cases where the proposed algorithm is used with parameterization u and b. The 'Pet' algorithm estimates 3 frequency components of the PN from the both sides of the direct current (DC) bin, with 3 iterations. 112 subcarrier symbol decisions are used per iteration to construct the PN estimate. These decisions are made so that the most reliable subcarriers are used based on the estimated channel amplitude response. These parameters enable reasonable performance, but the complexity is still significantly higher than in the proposed algorithm.

For both SU-MIMO and MU-MIMO cases, simulations are carried out with Matlab based 5G NR specifications compliant tool. We consider 2x2 SU-MIMO DL with spatial multiplexing of 2 streams. The SU-MIMO results are evaluated with code rates of 3/4 and 4/5 for 64QAM, and turbo codec implementation following [14]. In the decoder, 8 max-log-MAP decoding iterations are used. In the DL SU-MIMO scenario, the transmitted pilot blocks are averaged across the spatial streams. In MU-MIMO, we consider UL case with similar parameters as in the SU-MIMO case, but now there are 2 UEs each utilizing individual spatial stream, so we cannot do any averaging as described in Section IV. We assume 3 km/h UE mobility for all the cases.

B. Results and Analysis

In Fig. 3, 2x2 SU-MIMO DL case is considered for 64QAM with code rate 3/4 in CDL-C (right set of curves) and CDL-D (left set of curves) channels. With the proposed algorithm, only the DC bin and either one ($u = 1$) or two ($u = 2$) frequency components from the both sides of the DC bin are estimated, and a single pilot block with varying amounts of subcarriers is used. In CDL-D case, some improvement over the CPE-only mitigation ('CPE m.') can be achieved with the 'Pet' reference algorithm of [2] at higher SNR regime. With the proposed algorithm in 2x2 SU-MIMO case with 1;12, 1;24, and 2;24 configurations, the
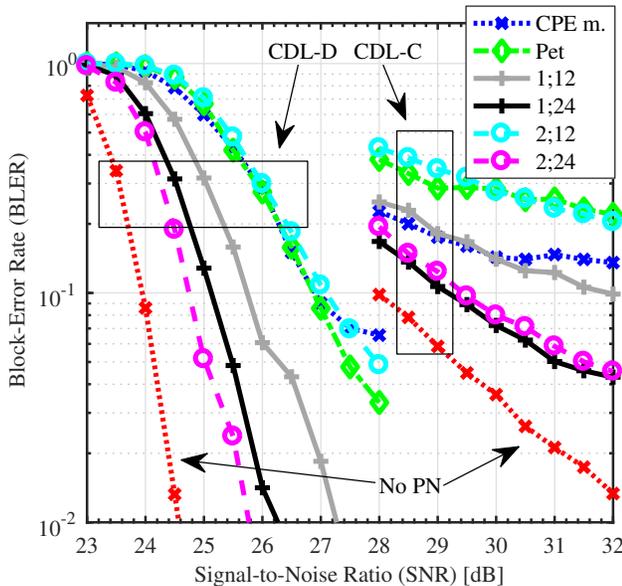
Fig. 3. Block-Error Rate as a function of signal-to-noise ratio in 2x2 SU-MIMO DL case for 64QAM (3/4) in CDL-C and CDL-D channels with 3 km/h mobility. In the legend entries for the proposed algorithm, $u;b$ defines the number of estimated ICI components per side and the pilot block length.

TABLE I. THROUGHPUTS [MBPS] IN CDL-D CHANNEL WITH 3 KM/H MOBILITY. LEFT-HAND SIDE COLUMNS AT 25.5-dB AND 64QAM (3/4) COMPARE SU-MIMO AND MU-MIMO CASES, AND RIGHT-HAND SIDE COLUMNS AT 26.5-dB COMPARE DIFFERENT CODE RATES IN SU-MIMO.

	25.5-dB SNR		26.5-dB SNR	
	2x2 MIMO	*2x2 MU-MIMO*	*64QAM (3/4)*	*64QAM (4/5)*
CPE m.	348	310	515	256
1;12	511	360	581	515
1;24	579	430	602	580
2;24	595	521	605	631
No PN	614	614	614	646

difference to the 'no PN' case is only around 1.7 dB, 1.2 dB and 0.7 dB, respectively, for the BLER target of 10%. Clearly in 2;12 case, the used 12 subcarrier block is too small for the $u = 2$ case, as it gives only performance similar to the reference algorithm. The CDL-C case is clearly more demanding for all the algorithms due to more frequency selective channel. Compared to the 'CPE m.' case, the considered 1;12 configuration offers performance improvement at the higher SNR range. Furthermore, the 1;24 configuration provides performance already within 1 dB of the ideal 'no PN' case at the 10% BLER target. With $u = 2$, the performance is slightly degraded and a larger pilot block size should be applied to benefit from larger u.

In the left two columns of the Table I, throughput results are given for 2x2 SU-MIMO and 2x2 MU-MIMO cases at 25.5-dB SNR in CDL-D channel. Notice that MU-MIMO throughput is evaluated as aggregated throughput of the two MU-MIMO users. The performance of the proposed algorithm is very good, in general, also in MU-MIMO, while the computational complexity stays very low. Furthermore, the *overhead is very small*, e.g., with a block of 12 pilots it is only 0.93%, and even with larger block size of 24, the overhead is only 1.9%. Notice that in Table I, the pilot overhead is taken into account.

In the right two columns of Table I, throughputs for the SU-MIMO case at 26.5-dB SNR for 64QAM with code rates 3/4 and 4/5 are given in CDL-D channel. In the PN free reference case, we can observe a clear improvement in the throughput with higher MCS. On the contrary, with CPE-only mitigation, or 1;12 and 1;24 ICI compensation schemes, the throughput is not improved due to increased sensitivity to PN and insufficient mitigation performance. With 2;24 ICI mitigation scheme, the throughput performance can be improved and it is very close to the PN free reference case, thus enabling the use of higher MSCs under PN. We thus notice that increasing the pilot overhead leads to improved throughput due to better PN estimation and compensation capabilities.

VI. CONCLUSION

When moving towards cmW and mmW frequencies in the emerging OFDM-based 5G and beyond systems, both the CPE and ICI induced by the oscillator PN needs to be considered and potentially suppressed through digital signal processing. In this paper, to facilitate symbol-by-symbol PN estimation and CPE+ICI compensation, a block type pilot allocation was proposed. Based on the proposed pilot allocation, a low-latency and computationally very efficient, yet highly accurate PN mitigation algorithm was formulated. It was shown through radio link simulations at 28 GHz carrier frequency that despite its simplicity, the proposed algorithm outperforms the existing state-of-the-art and can suppress the PN effects near to the PN free reference case in base station and mobile transceivers. The proposed scheme enables the use of higher MCSs, and was shown to be able to significantly improve the overall radio link throughput despite the involved pilot overhead.

REFERENCES

[1] T. Schenk, *et al.*, "Distribution of the ICI term in phase noise impaired OFDM systems," *IEEE Trans. Wireless Commun.*, vol. 6, no. 4, Apr. 2007.

[2] D. Petrovic, W. Rave, and G. Fettweis, "Effects of phase noise on OFDM systems with and without PLL: characterization and compensation," *IEEE Trans. Commun.*, vol. 55, no. 8, Aug. 2007.

[3] V. Syrjälä and M. Valkama, "Analysis and mitigation of phase noise and sampling jitter in OFDM radio receivers," *Int. Journal of Microwave and Wireless Technologies*, vol. 2, no. 2, pp. 193-202, Apr. 2010.

[4] N. N. Tchamov, *et al.*, "Enhanced algorithm for digital mitigation of ICI due to phase noise in OFDM receivers," *IEEE Wireless Commun. Lett.*, vol. 2, no. 1, Feb. 2013.

[5] V. Syrjälä and M. Valkama, "Iterative receiver signal processing for joint mitigation of transmitter and receiver phase noise in OFDM-based cognitive radio link," in *Proc. Int. Conf. on Cogn. Radio Oriented Wireless Netw. 2012*, Stockholm, Sweden, Jun. 2012.

[6] P. Mathecken, T. Riihonen, S. Werner, and R. Wichman, "Phase noise estimation in OFDM: Utilizing its associated spectral geometry," *IEEE Trans. Signal Process.*, vol. 64, no. 8, Apr. 2016.

[7] P. Rabiei, *et al*, "A non-iterative technique for phase noise ICI mitigation in packed based OFDM systems," *IEEE Tans. Signal Processing*, vol. 58, No. 11, Nov. 2010.

[8] J. Gozalvez, "5G Worldwide Developments," *IEEE Veh. Technol. Mag.*, vol. 12, no. 1, Mar. 2017.

[9] 3GPP TR 38.802 V14.2.0, Study on New Radio access technology; Physical layer aspects, Sep. 2017.

[10] 3GPP TS 38.214 V15.1.0, NR; Physical layer procedures for data, Apr. 2018.

[11] N. N. Tchamov, *Circuit- and System-Level Design of OFDM Receivers in the Presence of Phase Noise*, D.Sc. dissertation, Tampere University of Technology, 2013.

[12] 3GPP TR 38.803 V14.2.0, Study on New Radio access technology; RF and co-existence aspects, Sep. 2017.

[13] 3GPP TR 38.901 V15.0.0, Study on channel model for frequencies from 0.5 to 100 GHz, June 2018.

[14] 3GPP TS 36.212 V14.5.1, E-UTRA multiplexing and channel coding, Jan. 2018.